Atmos. Chem. Phys. Discuss., 7, 12145–12184, 2007
www.atmos-chem-phys-discuss.net/7/12145/2007/

Atmospheric Chemistry and Physics Discussions

Chemical composition of free tropospheric aerosol for PM1 and coarse mode at the high alpine site Jungfraujoch

J. Cozic[1], B. Verheggen[1,*], E. Weingartner[1], J. Crosier[2], K. Bower[2], M. Flynn[2], H. Coe[2], S. Henning[3], M. Steinbacher[4], M. Collaud Coen[5], A. Petzold[6], and U. Baltensperger[1]

[1]Laboratory for Atmospheric Chemistry, Paul Scherrer Institut, CH-5232 Villigen PSI, Switzerland
[2]School of Earth, Atmospheric and Environmental Sciences, University of Manchester, M60 1QD, UK
[3]Leibniz-Institute for Tropospheric Research, 04318 Leipzig, Germany
[4]Empa, Laboratory for Air Pollution/Environmental Technology, 8600 Dübendorf, Switzerland
[5]Federal Office of Meteorology and Climatology, MeteoSwiss, Aerological Station, 1530 Payerne, Switzerland
[6]Institute for Atmospheric Physics, German Aerospace Centre, 82234 Wessling, Germany
[*]now at: Energy research Centre of the Netherlands ECN, P.O. Box 1, 1755 ZG Petten, The Netherlands

Received: 6 July 2007 – Accepted: 8 August 2007 – Published: 17 August 2007

Correspondence to: E. Weingartner (ernest.weingartner@psi.ch)

Abstract

The chemical composition of submicron (fine mode) and supermicron (coarse mode) aerosol particles has been investigated since 1999 within the GAW aerosol monitoring program at the high alpine research station Jungfraujoch (3580 m a.s.l., Switzerland). Clear seasonality was observed for all major components in the last 9 years with low concentrations in winter (predominantly free tropospheric aerosol) and higher concentrations in summer (enhanced vertical transport of boundary layer pollutants). In addition, mass closure was attempted during intensive experiments in March 2004, February–March 2005 and August 2005. Ionic, carbonaceous and refractory components of the aerosol were quantified as well as the PM1 and coarse mode total aerosol mass concentrations. A relatively low conversion factor of 1.8 for organic carbon (OC) to particulate organic matter (OM) in winter (February–March 2005) was found. Organics, sulfate, ammonium, and nitrate were the major identified components of the fine aerosol fraction, while calcium and nitrate were the two major measured components in the coarse mode. The aerosol mass concentrations for fine and coarse mode aerosol during the intensive campaigns were not typical of the long term seasonality due largely to dynamical differences. Average fine and coarse mode concentrations during the intensive field campaigns were 1.7 $\mu g\,m^{-3}$ and 2.4 $\mu g\,m^{-3}$ in winter and 2.5 $\mu g\,m^{-3}$ and 2.0 $\mu g\,m^{-3}$ in summer, respectively. The mass balance of aerosols showed higher contributions of calcium and nitrate in the coarse mode during Saharan dust events (SDE) than without SDE.

1 Introduction

Atmospheric aerosol particles play an important role in global climate forcing. The aerosol chemical composition and size distribution are important in quantifying their radiative climate effects by means of absorption and scattering. The size and composition also influences the hygroscopic properties of the aerosol particles and their ability

to act as cloud condensation nuclei, and therefore affects cloud formation. Aerosol particles can also participate in heterogeneous reactions in the atmosphere, which are both composition and morphology dependant.

Measurements of size resolved chemical information can provide information on the sources of aerosol particles. Primary/secondary and anthropogenic/natural aerosol particles can have significant chemical and physical differences. Size discrimination into a coarse mode (particles with a diameter $d > 1\,\mu$m) and a fine mode (PM1;$d < 1\,\mu$m) is often applied. Primary aerosol refers to particles that are directly released into the atmosphere in the particle phase. Primary natural aerosol such as sea-salt, dust or volcanic ash particles typically belong to the coarse mode. Primary anthropogenic particles have various sources (black carbon (BC) for example is emitted by combustion processes) and often found primarily in the fine mode. Secondary aerosol is formed by transformation of gaseous precursors (both from natural or anthropogenic sources) into condensable material. For example sulfate can be found as natural secondary aerosol originating from oxidation of dimethyl sulfide released from marine plankton (Charlson et al., 1987), or anthropogenic secondary aerosol from the oxidation of SO_2. (Colbeck, 1998) which is emitted in large concentrations from fossil fuel power stations. Automobiles, industry, cooking and combustion are examples of anthropogenic sources of aerosol precursor gases. Secondary aerosol typically represents the majority of the fine particle mass (Turpin and Huntzicker, 1995).

The main constituents of fine atmospheric aerosol are inorganic ions, organic compounds and to a lesser extent black carbon (BC) otherwise known as elemental carbon (EC)(Krivacsy et al., 2001). While inorganic ion species and their concentrations have been determined at many locations around the world, data for carbonaceous compounds are rather limited due to the lack of instrumentation allowing for the artifact free quantification of organic fraction. In the recent years new instrumentation (aerosol mass spectrometry, thermal-optical carbonaceous analyzers) became available allowing the quantitative determination of the organic fraction, which comprises the dominant fraction of the fine aerosol in various environments (Zhang et al., 2007).

Knowledge of the chemical composition of atmospheric aerosol is important to assess its impact on the environment. Presented in the following are long-term measurements of the chemical composition of coarse and fine mode aerosol particles from 1999 to 2006 at the high-alpine site Jungfraujoch, in the Swiss Alps. The mass closure for PM1 and coarse mode aerosol during intensive field measurements performed in March 2004, February–March 2005 and August 2005 is also investigated. Following instrument intercomparisons, mass fractions of the various components for different seasons and aerosol types are discussed as well as their partitioning into the different size fractions.

2 Site, sampling and analysis

Measurements have been performed within the Global Atmosphere Watch (GAW) aerosol program of the World Meteorological Organization since 1999 and more intensively during Cloud and Aerosol Characterization Experiments (CLACE) at the high-alpine research station Jungfraujoch (Switzerland, 3580 m a.s.l.). The intensive field campaigns took place in March 2004, from mid July to end of September 2004, from mid February to mid March 2005 and in August 2005.

2.1 Jungfraujoch station

The Jungfraujoch (JFJ) measurement site is located on an exposed mountain saddle in the Swiss Alps at 3580 m a.s.l. Atmospheric aerosols and gases have been measured at the JFJ within the GAW program for over a decade. The station is regularly engulfed in clouds (37% of the time based on a year long survey by Baltensperger et al., 1997). Due to its elevation, the site is only weakly influenced by local anthropogenic sources. These characteristics make the Jungfraujoch well suited to investigate continental background aerosols and clouds from a ground based platform.

Measured aerosol parameters at the Jungfraujoch exhibit a strong seasonal cycle

with a maximum in summer and a minimum in winter. In summer, the site is influenced by injections from planetary boundary layer air during afternoons with high solar insulation or during frontal activity, leading to variations in the concentrations and properties of the aerosol measured. Reduced solar heating in winter reduces the extent of vertical mixing and results in substantially lower aerosol concentrations (Weingartner et al., 1999; Henne et al., 2005). Therefore, the site is deemed representative of the lower free troposphere above a continental area. More information on the Jungfraujoch site and the long term aerosol measurements can be found in Baltensperger et al. (1997) and Collaud Coen et al. (2007). Table 1 summarizes the different types of instruments operated during the different campaigns.

2.2 Inlet

The standard GAW total aerosol inlet was used at the JFJ, which is heated to 25°C to evaporate cloud droplets and ice crystals at an early stage of the sampling process. This inlet was designed to sample cloud droplets smaller than 40 μm at a wind speed up to 20 m s^{-1} (Weingartner et al., 1999). The aerosol sample thus consists of aerosols incorporated into cloud droplets, ice crystals, and un-activated (interstitial) aerosols. Following passage through the inlet, the aerosol particles are sampled at laboratory room temperature and are considered dry (relative humidity <20%).

2.3 Black carbon measurements

The Multi-Angle Absorption Photometer (MAAP, Thermo ESM Andersen) (Petzold and Schonlinner, 2004) measures the transmitted and backscattered light intensity from a defined source (λ=630 nm) incident on a fiber filter, through which air is also drawn. The particle light absorption coefficient b_{abs} is obtained from a radiative transfer scheme which corrects for artifacts caused by the interaction of the light with the filter material. The instrument is used to measure the black carbon mass concentration (BC) in real time. Black carbon (BC) is the most efficient light-absorbing aerosol

species in the visible spectral range. Thus, the aerosol light absorption in the visible spectral range is strongly correlated with the concentration of black carbon. The relationship between the aerosol absorption coefficient b_{abs} (m^{-1}) and the corresponding black carbon mass concentration BC (g m^{-3}) is established by a mass absorption efficiency $\sigma_{abs,BC}$ (m^{2}g^{-1}) via the relationship

$$b_{abs}=BC\cdot\sigma_{abs,BC} \quad (1)$$

where $\sigma_{abs,BC}$ and b_{abs} are wavelength dependent. $\sigma_{abs,BC}$ depends on the type of aerosol, the aging and the size of the BC particles (Liousse et al., 1993) and thus needs to be determined for each site. In the following, a value of 7.4 m^{2}g^{-1} was used in winter and 10.8 m^{2}g^{-1} in summer at 630 nm as detailed in Sect. 3.1.2. Measurements were performed with a time resolution of 1 min. Comparison with another MAAP instrument running behind a PM2 inlet showed a very high correlation (r^2=0.97) indicating that most of the BC mass is found below d=2 μm (Cozic et al., 2007).

2.4 Semi-continuous OC/EC thermo-optical analyzer

Organic carbon (OC) and elemental carbon (EC) in the total suspended particulate matter (TSP) were measured using a semi-continuous OC/EC thermo-optical transmission analyzer (Sunset Laboratory) (Birch and Cary, 1996; Bae et al., 2004). Sample matter is accumulated for 5 h 45 min (flow rate=7.5 L min^{-1}) on a quartz filter within the instrument after passing through a gas phase denuder (charcoal-impregnated filter strips, Sunset Laboratory) (Bae et al., 2004). The filter was then heated in an oxygen-free ultra high purity helium atmosphere in four increasing temperature steps, which permits the detection of various organic carbon fractions. During these heating steps some organic compounds may be pyrolytically converted to EC. This pyrolytic conversion was continuously monitored by measuring the transmission of a laser beam (λ=660 nm) through the filter. The organic compounds were vaporized and oxidized to carbon dioxide by a manganese dioxide catalyst at 800–900°C. Then the gas was

switched to a 2% O_2/He mixture and the filter was heated in two increasing temperature steps for determination of EC. In both cases, the produced CO_2 was continuously quantified by non-dispersive infrared absorption (NDIR). At the end of each analysis an automatic internal calibration was done by using a known volume and concentration of methane (5% CH_4; 95% He). A second calibration was also provided off-line at the beginning and end of each campaign with an external source of methane gas injected during the He/O_2 phase.

The determined EC includes both the original EC and that produced by the pyrolysis of organics. The point where the laser beam transmission through the sample returned to the original sample transmission was used to define the split between organic and elemental carbon (the instrument response prior to this point being assigned to OC and after this point assigned to EC). This split point was always estimated automatically by the instrument for the distinction between EC and pyrolized OC. The main difficulty is the correct separation between EC and OC: several temperature programs and results of intercomparison exercises are described in the literature (Chow et al., 2001; Schmid et al., 2001; Schauer et al., 2003). Theses studies generally show that the sensitivity of the separation between EC and OC using a TOT (transmission) analysis method depends mainly on the temperature program and on the type of samples analyzed. It has been observed at JFJ that the split point was quite often in the last OC fraction and the pyrolized fraction was small.

The analyses were based on a temperature program provided by NIOSH (National Institute for Occupation Safety and Health): temperature up to 840°C for the analysis of OC in 100% He (1st step: 310°C for 60 s; 2nd step: 480°C for 60 s; 3rd step: 615°C for 60 s; 4th step: 840°C for 90 s), and up to 850°C for the analysis of EC in 98% He + 2% O_2(1st step: 550°C for 35 s; 2nd step: 850°C for 105 s).

2.5 Chemical composition of aerosol filter samples

The filter sampling system was designed to sample two size classes, Total suspended particles (TSP) and particles with an aerodynamic diameter $d<1\,\mu$m (PM1)

(Henning et al., 2003). The two sizes classes were selected according to the recommendations of the Global Atmospheric Watch (GAW) scientific advisory group for aerosol, reflecting the fact that the mass scattering efficiency is quite different for submicron and supermicron aerosols (Finlayson-Pitts and Pitts, 2000; GAW, 2007; IPCC, 2007). Four stages of a cascade impactor (Maenhaut et al., 1996) were used to generate the cut-off of $d=1\,\mu$m with a flow rate of 11 L min^{-1}. The flow was controlled by a mass flow controller (5851E Brooks Instrument, Fisher-Rosemount AG). The impactor stages were treated with high-vacuum grease to prevent bouncing. More details on the sampling system can be found in Henning et al. (2003).

Teflon filters (PTFE, Sartorius AG) with a pore size of 1.2 μm and 47 mm diameter were used to sample the particulate matter, and Nylon filters (Nyabsorb, PALL/Gelman Sciences) with a pore size of 1 μm were used for collection of nitrate, which might evaporate from the first filter (Zhang and McMurry, 1992; Cheng and Tsai, 1997). Cleaning of the filters with deionized water, NaOH or methanol was found to be not necessary because of the low blank values of the filters, which were tested regularly. All filters were stored in Petri dishes lined with baked aluminum foil liners and placed in sealed polyethylene bags. All filters were stored at −18°C until their analysis.

Samples were analyzed for water soluble ionic components with ion chromatography in a clean room 0.1 for particles $d<0.1\,\mu$m. Filters were extracted in SCHOTT bottles, for Teflon filters using 0.3 mL of methanol (Baker CMOS grade) in order to first wet the Teflon filters, followed with 8.7 mL of deionized (DI) water and for Nylon filters with 5mL of DI water. Extracts were analyzed within 1 h after this procedure in order to limit possible oxidation reactions in the liquid phase. Cations (Na^+, NH_4^+, K^+, Mg^{2+}, Ca^{2+}) were analyzed with a DIONEX DX320 chromatograph using a CS16 column with a CG16 guard column, and chemical regeneration was made with a CSRS ULTRA II autosuppressor using a 0.6 mL injection loop and a MSA gradient. Anions were analyzed in parallel with a DIONEX ICS 2500 chromatograph using an AS11 column with an AG11 guard column and an ASRS ULTRA II autosuppressor. Injection was performed with a 1 mL injection loop, and a KOH gradient with an EG50 eluent generator. The 15-min

runs allowed for the detection of the major inorganic anions (Cl^-, NO_3^-, SO_4^{2-}) and a suite of species including organic acids.

Blank levels for each chemical species were calculated from the analysis of 30 procedural blanks and were subtracted from the measured samples concentrations to obtain the actual concentrations. Atmospheric detection limits were calculated as twice the standard deviation of the blank sample concentrations, using a typical sampling duration of 24 h. Major components (sulfate, chloride, sodium, ammonium, nitrate, potassium and magnesium) were almost always above detection limit. The chemical composition of the coarse mode particles was calculated by the difference between TSP and PM1 data.

Aerosol nitrate is difficult to determine due to possible sampling artifacts. As explained by Henning et al. (2003), gaseous nitric acid was assumed to be quantitatively lost during transport through the inlet system (4.5 m length, 11 s residence time). Any nitrate measured on the backup Nylon filter was assumed to originate from ammonium nitrate. In the following, NO_3^- is presented as the sum of nitrate from the Teflon and the Nylon filter in order to get the total aerosol nitrate. For NH_4^+, the total ammonium concentration was obtained by the addition of the ammonium determined on the Teflon filter plus an equivalent amount of ammonium estimated from the associated nitrate on the backup filter.

2.6 Aerosol Mass Spectrometer

An Aerodyne Quadrupole Aerosol Mass Spectrometer (Q-AMS, Jayne et al., 2000) was used for measuring on-line chemically resolved mass concentrations and size distributions of non-refractory aerosol components (sulfate, nitrate, ammonium, organics), in the size range of d=50–700 nm. In the Q-AMS, the particles are drawn into vacuum through a unique aerodynamic lens sampling inlet system (Liu et al., 1995a,b; Zhang et al., 2002), which focuses aerosol particles into a narrow, collimated beam that impacts on a porous tungsten surface (the vaporizer) heated typically to 500˚C under high vac-

uum ($\sim 10^{-8}$ torr). The non-refractory fraction of the particles, mostly the volatile and semi-volatile components, flash vaporize upon contact with the vaporizer surface on a time scale of a few microseconds. The resultant gaseous molecular constituents are then ionized using a 70-eV electron impact ionization source positioned such that the maximum electron density and the centre of the vaporized plume are co-located in the extraction zone of the mass spectrometer. A quadrupole mass spectrometer (QMA 410, Balzers Instruments, Balzers) is utilized to analyze the positive ions with unit mass-to-charge (m/z) resolution. For more details see Allan et al. (2003).

2.7 Particle size distribution measurements

A scanning mobility particle sizer (SMPS, TSI 3934), comprising a differential mobility analyzer (DMA, TSI 3071) and condensation particle counter (CPC, TSI 3022), was used to measure the particle size distribution between 17 and 900 nm (dry) diameter (Verheggen et al., 2007). The SMPS employed a closed loop configuration for the sheath and excess air flow rates, which were held constant at 3 L min^{-1} by a critical orifice, while the sample flow was 0.3 L min^{-1}. The diameter was corrected for the reduced pressure at the Jungfraujoch (650 mbar on average). The correct sizing of particles was confirmed by means of latex calibration spheres. The SMPS was frequently compared to another SMPS and systematic differences in integrated concentrations <5% were encountered. The measured SMPS number size distributions were used to derive an aerosol volume concentration of particles with d<900 nm by assuming spherical particles.

Additionally, an optical particle counter (OPC, Grimm Dustmonitor 1.108) was running to measure the particle size distribution in the optical diameter range d=0.3-20 μm. The intercomparison with the size distribution spectrum of the SMPS showed a very good agreement for February–March 2005 whereas for March 2004 the OPC diameters would need to be slightly shifted (multiplied by 1.2) to larger sizes to get a good agreement. The slight discontinuity in the combined number size distribution

is likely to result from the fact that in the OPC the individual particles are classified according to their light scattering behavior, which depends on the particle size, morphology and refractive index. Since the OPC is calibrated with spherical Latex particles the observed shift is most probably due to the different refractive index (and complex morphology) of the measured particles in the range d=300–1000 nm.

2.8 Betameter TSP and PM1

A beta-attenuation monitor (Thermo ESM Andersen FH62 I-R) was used for continuous measurements of TSP and PM1 mass concentration (Baltensperger et al., 2001). Particles are sampled on a glass fiber filter exposed to a continuous flux of beta particles. The beta particles are emitted as a continuum energy distribution by a radioisotope source and the intensity of their transmission through a reference section and through the sample is measured by an electron counter. The number of beta particles transmitted through the sample decreases exponentially as the thickness of the deposited material increases according to Evans (1955),

$$I = I_0 \cdot e^{-\mu \cdot x} \quad (2)$$

where I_0 is the incident flux, μ is the mass absorption coefficient for β radiation absorption ($cm^2\ g^{-1}$), and x is the mass thickness of the sample ($g\,cm^{-2}$). The mass absorption coefficient is determined through a calibration procedure involving the measurement of a series of known standards (calibration foils), which bracket the mass range of interest (Jaklevic and Gatti, 1981).

2.9 High-volume sampler for TSP

A high-volume sampler (HIVOL DHA80, Digitel, Hegnau) was used to determine 48 h-averages of total suspended mass concentrations. TSP was collected for 2 days on glass fiber filters (Ederol 227/1/60, diameter 15 cm, Digitel) with a flow rate of 45 $m^3\ h^{-1}$. The mass concentrations were determined gravimetrically by weighing the filters

before and after sampling (Mettler, AE200). From January 2006 onwards, sampling intervals were reduced to 24 h and glass fiber filters were replaced by quartz fiber filters (QMA20, Whatman, Dassel).

2.10 Nephelometer

The aerosol light scattering coefficients of TSP are simultaneously measured at three wavelengths (λ=450, 550, and 700 nm) by an Integrating Nephelometer (IN, TSI 3563). The sampled aerosol is illuminated over an angle of 7 to 170° by a halogen light source directed through an optical pipe and opal glass diffuser. The sample volume is viewed by three photomultiplier tubes through a series of apertures set along the axis of the main instrument body. Aerosol scattering is viewed against the dark backdrop of a very efficient light trap.

3 Results

3.1 Measurement Validation

3.1.1 Mass absorption efficiency

The mass absorption efficiency $\sigma_{abs,BC}$ of the Jungfraujoch aerosol was determined from the EC measurements of the OC/EC analyzer and the light absorption measurements (MAAP). $\sigma_{abs,BC}$ is wavelength dependent and is determined here for λ=630 nm. A large range of values (2–25 $m^2 g^{-1}$) has been reported in the literature (Bond and Bergstrom, 2006) and references therein. This variability may be partly caused by differences in the aerosol mixing state, with external mixtures favoring smaller values, while larger values indicate internal mixing of BC Liousse et al., 1993. Consequently, $\sigma_{abs,BC}$ is dependent on the aerosol composition, mixing state and to a lesser extent particles size. However, it is believed that a major contribution to this wide range is

caused by the variability in the different methods to determine EC and BC (Schmid et al., 2001).

Figure 1 shows the comparison between the absorption coefficient b_{abs} measured by the MAAP with the EC concentration determined by the OC/EC analyzer in February–March 2005 and in August 2005. The indicated slopes in the graphs were determined by orthogonal regression taking into account the error of each instrument and generating noise in the data to estimate the error on the mass absorption efficiency. The mass absorption efficiency is higher in summer ($11.1 \pm 0.2\,m^2 g^{-1}$) compared to winter ($7.6 \pm 0.2\,m^2 g^{-1}$). The reasons for this difference are currently unclear but might be explained by a greater coating of BC particles by e.g. organic compounds due to increased photochemical activity during summer. Such coatings may lead to increases in mass absorption efficiency (Fuller et al., 1999). This seasonality in the mass absorption efficiency has been seen in other studies such as Sharma et al. (2002) in the Canadian Arctic, but not in a previous study at the Jungfraujoch (Lavanchy et al., 1999). The later may be due to different procedures used in the different campaigns.

3.1.2 Q-AMS Collection Efficiency

Due to collection efficiencies of ambient particles of less than 100% within the aerosol mass spectrometer, the Q-AMS data have to be corrected. The collection efficiency correction arises from the fact that particles with large amounts of non-volatile mass (such as ammonium sulfate) can bounce off the Q-AMS heater without evaporating, meaning they are not measured. The data for the non-refractory aerosol components (such as SO_4^{2-}) were compared to the filter data in order to estimate the collection efficiency of the Q-AMS.

Figure 2 shows the comparison of the SO_4^{2-} concentrations measured with the Q-AMS and on the filters. The slope of the linear correlation equation yields the AMS collection efficiency. A collection efficiency of 0.48 was found for sulfate. Since the aerosol in the fine mode has been shown to be mainly internally mixed at Jungfraujoch (Weingartner et al., 2002; Cozic et al., 2007), the collection efficiency of 0.48

was applied to all compounds (SO_4^{2-}, NO_3^-, NH_4^+, organics) measured by the Q-AMS. The coefficient is consistent with values found in previous studies (Canagaratna et al. (2007) and references therein).

3.1.3 Organic Matter (OM) and Organic Carbon (OC)

The OC/EC analyzer measures organic carbon (OC) and does not consider the other atoms associated with organic matter, such as O, H, N and S. In contrast, the organic mass concentration from the Q-AMS represents the total organic matter (OM) associated with all atoms present. The comparison between these two concentrations yields information on the conversion factor of OC to OM for the Jungfraujoch aerosol. This comparison was only possible in February–March 2005 when the Q-AMS and the Sunset analyzer were sampling simultaneously. As mentioned above, the organic mass concentration from the Q-AMS was corrected for collection efficiency. An offset correction was applied to the OC concentration found with the Sunset analyzer, as a detailed analysis revealed an offset in the Sunset data of about $0.3\,\mu g\ m^{-3}$. Tests were performed in the laboratory with Nitrogen (quality 5.0) and further purified with a pure air generator (AADCO Instruments Inc., 737–250 series). According to the manufacturer's specifications impurities were <1 ppb each for ozone, methane and non-methane hydrocarbons, oxides of nitrogen (NO/NO_x), hydrogen sulfide (H_2S), sulfur dioxide (SO_2), carbonyl sulfide (COS), carbon monoxide (CO), sulfur hexafluoride (SF_6), and fluorocarbons. In addition a particle filter and a denuder were installed in front of the instrument inlet to remove particles and semi volatile gases from the air. The resulting "clean air" showed that this offset did not increase with sampling time (up to 24 h) and was only present in the first two steps of OC temperature program. No clear reason of this offset was found since a leak or penetration of compounds through the denuder would have resulted in a blank that is dependent on sampling time. These offsets were estimated to 0.2 and 0.1 μg for the 1st and 2nd peaks, respectively, and were subtracted from the respective peaks measured in the field.

As can be seen in Fig. 3 there is a high correlation between the OC and the OM (r^2=0.89) and the conversion factor of OC to OM is 1.84. This finding is in agreement with literature data where values between 1.6 to 2.1 have been reported (Turpin and Lim, 2001). An even higher factor might be expected for the Jungfraujoch aerosol due to its remote location. Nevertheless during this campaign quite high aerosol concentrations were observed indicating the influence of relatively fresh aerosol. This coefficient could be slightly decreased by the site cut of 1 μm used for the Q-AMS whereas the OC/EC analyzer was running with TSP. This is not expected to have a strong influence at the JFJ. In the following the same coefficient will be used for winter and summer since no Q-AMS was running during the summer period. In summer this coefficient is expected to be higher due to the larger biogenic emissions and increased photochemical activity.

3.1.4 Betameter PM1 and SMPS mass concentration

The PM1 data from the betameter have very low signal to noise ratios unless they are averaged over sufficiently long periods (typically 1 day). A higher temporal resolution of PM1 can be estimated by correlating the PM1 data (24-h averages) with the volume concentrations obtained from the measured SMPS size spectra (d=17–900 nm) and estimating an aerosol density. Although there are a large number of particles with d<17 nm, these small particles can be neglected when calculating the submicrometer aerosol volume concentration (Imhof et al., 2005). The missing aerosol volume between 900 and 1000 nm can also be considered as negligible when strong episodes of mineral dust are absent, as shown in the size distributions below (Sect. 3.4).

Figure 4 shows the comparison of the PM1 mass concentration with the submicrometer aerosol volume for March 2004, February–March 2005, and August 2004 (24 h averaging time). The correlation shows some scatter (r^2=0.53) which is explained with the low signal to noise ratio of the betameter. The conversion factor corresponds to an effective particle density of 1.5 g cm^{-3} which is consistent with the values observed at Monte Cimone (Putaud et al., 2004b), Hyytiälä (Virtanen et al., 2006) and those

summarized by McMurry et al. (2002). Thus we conclude that it is appropriate to estimate the PM1 mass concentration from the SMPS volume concentration when SMPS measurements were available (winter campaigns) by using an effective particle density of 1.5 g cm^{-3}. In summer the concentrations were higher, resulting in higher signal to noise ratios in the betameter data so that they could be used directly.

3.1.5 Betameter TSP and Gravimetric TSP

The correlation between the two TSP measurements (Fig. 5a) is high (r^2=0.94), with a slope slightly higher than one ($TSP_{betameter}$=1.12 $TSP_{gravimetric}$). The slightly high slope could be due to a calibration issue for the betameter at the Jungfraujoch. The comparison between the betameter data for TSP and PM1 (Fig. 5b) reveals that the signal of the PM1 betameter is much lower than TSP betameter as expected ($TSP_{betameter}$=1.58 $PM1_{betameter}$), but is also noisier and yields a lower correlation (r^2=0.41). Episodes of Saharan dust (yellow points on Fig. 5b determined by the method described by Collaud Coen et al., 2004) were excluded from the correlation, since they show much higher concentrations of coarse mode particles .

3.1.6 Long-term chemical composition

Since June 1999 inorganic compounds in PM1 and TSP have been determined on a semi-continuous basis (24 h sampling every 6th day) on the JFJ within the GAW aerosol program. Long-term ionic measurements at a various European sites have been published by Putaud et al. (2004a). However, only annual averages are presented for fewer components Malm et al. (2004) presented a summary of monthly evolutions for different sites within the US. They showed temporal evolutions over a year but no year to year evolution was discussed. Long-term series are available for individual components such as sulfate (e.g., Malm et al., 2002). This paper is to our knowledge the longest time series of inorganic aerosol composition at a remote site presented so far. In addition the mass concentrations of PM1 and TSP have been measured

since February 2004 and June 1999 respectively. Figure 6 presents the long-term measurements of the major PM1 and TSP compounds detected (SO_4^{2-}, NH_4^+, NO_3^-, Ca^{2+}, K^+, $C_2O_4^{2-}$, Mg^{2+}, Cl^-, Na^+), as well as the TSP mass concentration determined by gravimetry and the PM1 mass determined with a betameter (since January 2004 only).

For all compounds a clear seasonality is observed with low concentrations in winter when the aerosol is typical of the undisturbed free troposphere and maximum concentrations in summer when the Jungfraujoch is influenced by injections from the planetary boundary layer (PBL). It can be seen that highest TSP mass concentrations were reached in summer 2003 when Europe encountered exceptionally high temperatures which led to increased convection and thus enhanced injection of PBL air. These high signals in summer 2003 were also observed in other continuous aerosol measured parameters such as the light scattering coefficients (Collaud Coen et al., 2007). However, of the chemical components measured, only NO_3^- showed significant enhancements.

No statistically significant trends in the major ionic species could be obtained from this data set in contrast to other aerosol parameters measured within the GAW program for which clear trends were observed (Collaud Coen et al., 2007). For the TSP mass during the period 1975 to 2005 a decrease in mass with time was observed. It was not possible to identify a significant trend for the last 9 years (Christoph Hüglin, personal communication). This might be explained by lower temporal coverage of the chemical composition samples (24 h sampling every 6 days instead of continuously as for the other parameters) which introduces some more uncertainties and from a higher year to year variation. This might mask a possible trend.

The different intensive campaigns are marked as orange bands in Fig. 6. It is clearly seen that there is a strong variability between the two winter campaigns. The period February–March 2005 presents unusually high concentrations for a winter period (e.g.~700 ng m^{-3} for SO_4^{2-} instead of <400 ng m^{-3} for winter in other years) and reaches concentrations similar to those found in summer. The campaign in August 2005 was performed after the maximum PBL influence at the JFJ. In addition, the

month of August 2005 was cool and cloudy which resulted in low influence from the PBL.

3.2 Aerosol neutralization

The degree of neutralization of the aerosol (PM1 only) is presented in Fig. 7, which shows the ratio of the measured NH_4^+ to the amount of NH_4^+ that is needed to neutralize nitric and sulfuric acid is shown, as a function of the total ion mass concentration. Each data point represents a single 24 h sample, with data from the entire 6 year dataset displayed. It appears that within the noise in the data the Jungfraujoch aerosol can be mainly estimated as neutralized, since the average ratio is about 80%. At low mass concentrations there is a slight tendency for increased acidity, but there is considerable scatter at these low concentrations. This tendency might be due to the fact that ammonia has a very strong gradient with altitude (Beig and Brasseur, 2000); thus a high degree of acidity may indicate an influence of free tropospheric air.

During the intensive field campaigns in March 2004, the aerosol was found to be substantially more acidic than in February–March 2005 and August 2005. As explained above, this might indicate an influence of free tropospheric air.

3.2.1 Chemical mass balance for PM1 and the coarse mode

Time series of the chemical mass balance for PM1 and coarse mode for three intensive field campaigns in March 2004, February–March 2005 and August 2005 are presented in Fig. 9. No mass closure is given for July–August 2004 since the organic mass concentration was not measured during this period.

Figure 9 presents the various measured chemical fractions as well as total PM1, total coarse and TSP mass concentrations. As explained in Sect. 3.1.4, the PM1 mass concentration was derived from the SMPS volume concentration for March 2004 and February–March 2005. In August 2005 no SMPS data were available. For this campaign, the aerosol light scattering coefficient at wavelength λ450 nm

was used as a proxy for the PM1 mass. The SMPS derived volume concentrations were compared to the measured aerosol light scattering coefficients at 450 nm. The analysis showed a high correlation (r^2= 0.71, slope= $5.95 \cdot 10^{-6}$ $m^{-1}cm^3\mu m^{-3}$ (March 2004); r^2=0.98, slope=$6.14 \cdot 10^{-6}$ $m^{-1}cm^3\mu m^{-3}$ (July–August 2004); r^2=0.94, slope=$6.92 \cdot 10^{-6}$ $m^{-1}cm^3\mu m^{-3}$ (February–March 2005)) between these parameters, justifying the use of the scattering coefficient as a PM1 proxy for August 2005.

It can be seen on Fig. 9 that the two fractions present a highly different chemical composition. The PM1 mode is mainly composed of organics and sulfate (SO_4^{2-}) along with significant fractions of BC, nitrate (NO_3^-), and ammonium (NH_4^+). The non-determined mass (ND) is quite small and is assumed to be composed of all insoluble compounds such as silicate from mineral dust. As mentioned previously, the aerosol is measured at laboratory temperatures (i.e. under dry conditions) and the ND fraction is therefore not expected to be explained by condensed water. In contrast, the coarse mode is dominated by the ND fraction. The major determined compound in the coarse mode is calcium (Ca^{2+}), which is a known component of mineral dust. The contribution of the measured inorganic compounds is very small, and nitrate seems to be present in the same proportion as sulfate. As shown by Krueger et al. (2004) NO_3^- can be linked with Ca^{2+} in the coarse mode by the reaction of mineral dust particles with nitric acid to form $Ca(NO_3)_2$. Other compounds (silica etc.) were not measured.

The large contributions of Ca^{2+} on 14 and 20 March in Fig. 9 are due to distinct episodes of Saharan dust over the Jungfraujoch region. These mineral dust episodes were confirmed by the method developed by Collaud Coen et al. (2004), where the wavelength dependence of the single scattering albedo (expressed as the SSA exponent) was found to be an indicator for the presence of dust particles. This exponent becomes negative in presence of mineral dust. For these two cases the ND fraction in PM1 can be explained by a substantial extension of the coarse mode size distribution into PM1 (Fig. 10), as also shown by Schwikowski et al. (1995).

During the March 2004 campaign the ND fraction in PM1 is surprisingly high, excluding periods when Saharan dust events were identified. As can be seen in Fig. 9,

this can not be explained by the presence of mineral dust since there is no elevated coarse mode and the SSA exponent is not negative. Figure 10 presents two typical volume size distributions from combined SMPS and OPC data during events where continental background aerosol without and with the influence of mineral dust particles was sampled. As explained in the instrumental part, the slight discontinuity in the combined number size distribution is likely to result from the difference of refractive index (and complex morphology) of the measured particles with the spherical Latex particles which are used to calibrate the OPC. In the absence of a calibration with the actual JFJ aerosol no correction was applied.

The high ND fractions observed in March 2004 were carefully checked for systematic biases. First, the SMPS derived volume concentrations were compared to the measured aerosol light scattering coefficients at 450 nm. As presented above these two parameters showed a very high correlation and virtually the same ratio (V_{SMPS} / b_{scat}) was determined during March 2004 compared to the other campaigns. This indicates that the aerosol volume is not a critical factor in the unexplained ND fraction. Second, to validate the chemistry data, the SO_4^{2-} measured with the filters was compared with the mass concentration of sulfate calculated from the sulfur data measured within the NABEL network. A good correlation between the two measured fractions (r^2=0.57; SO_4 (PSI)=$0.81 \cdot SO_4$ (NABEL)) was found which indicates that the concentrations of the filters were correct. Thus the ND fraction could originate either from an unknown component or from a non-identified problem.

In addition to the size distribution, 48-h back-trajectories were calculated with the NOAA HYSPLIT model (Draxler and Rolph, 2003) for the two periods shown in Fig. 10. The different colors represent the back-trajectories starting at 2 h (Fig. 10a) and 3 h-intervals (Fig. 10b). The bottom panel shows the altitude of the back-trajectories given in altitude above ground level (a.g.l.). The JFJ is only situated at about 1450 m a.s.l. in the model due to the limited resolution of the model topography. In consequence, the starting point of the back-trajectories is taken at 2130–2160 m a.g.l. (in contrast to the 3580 m a.s.l.). These back-trajectories confirm the influence of dust on 13–14 March

as the air mass came from the Saharan region and reached the ground in this region. On 6–7 March the air mass came from to the area above the UK and across France at an altitude of ∼2000 m a.g.l., which gave a clean background air.

For the period between 25 February and 10 March 2005, the concentrations of individual species were exceptionally high for this time of the year and close to summer values, when the Jungfraujoch is influenced by injection of PBL layer air into the lower free troposphere. This is also confirmed by an observed scattering coefficient (at 450 nm) during this time period of $1.2{\cdot}10^{-5}$ m^{-1} compared to $3.2{\cdot}10^{-6}$ m^{-1} as the long-term average (years 1995 to 2006) for this time period of the year. The reason for these high concentrations is presently unknown. The contribution of mineral dust to PM1 was small during this time period as confirmed by an analysis of SSA exponent and OPC size distributions (not shown).

The last campaign presents a summer situation when the site is influenced by the PBL. Much higher organic fractions in PM1 were observed than in winter, as expected since biogenic emissions and photochemistry are enhanced in summer. The PM1 mass presents negative values due to the low signal to noise ratio of the betameter used here since no SMPS data were available.

Figure 11 presents the averages of the chemical composition for the three campaigns as pie charts. These pie charts confirm the highly different composition of fine and coarse mode particles, as well as the higher organic fraction in summer compared to winter. The two winter campaigns are quite different, with a much higher non-determined fraction in PM1 in March 2004. In contrast, the February–March 2005 was a period with a much higher concentration of water soluble inorganic species, as outlined above. In March 2004 the mean average concentrations of the fine and coarse mode were 1.7 $\mu g\,m^{-3}$ and 2.4 $\mu g\,m^{-3}$, respectively, whereas they were 2.0 $\mu g\,m^{-3}$ and 0.9 $\mu g\,m^{-3}$ during February–March 2005.

4 Conclusions

The chemical composition of PM1 and TSP has been investigated since 1999 within the GAW aerosol program at the high alpine site Jungfraujoch. A clear seasonality in all inorganic compounds was observed with minima in winter typical of the undisturbed free troposphere and maxima in summer where the site is influence by injections of boundary layer air. In addition, intensive campaigns permitted a chemical mass closure of PM1 and the coarse mode to be performed. These two fractions present highly different chemical composition, with PM1 dominated by organics, sulfate, nitrate, ammonium, BC and the coarse mode composed of mainly ND and calcium, along with minor fractions of nitrate and sulfate. A clear influence of mineral dust episodes was observed in the coarse mode. A conversion factor from OC to OM of 1.84 in winter was found, which is within the range of values reported in the literature.

Acknowledgements. We thank the International Foundation High Altitude Research Stations Jungfraujoch and Gornergrat (HFSJG) for the opportunity to perform experiments on the Jungfraujoch. We are grateful to the custodians at Jungfraujoch (Families Staub, Hemund and Fischer) for their inspection and maintenance of instrumentation. The financial support of MeteoSwiss (Global Atmosphere Watch, GAW) is highly appreciated. We thank J. L. Jaffrezo for allowing us to use his ion chromatography facilities at LGGE Grenoble. Parts of the ion chromatography analyses were performed by TERA Environnement, Bernin, France. We thank the UK NERC for the AMS measurements support through research grants NER/A/S/2003/00541, NER/A/S/2001/01135 and NERC studentship NER/S/A/2003/11441.

References

Allan, J. D., Alfarra, M. R., Bower, K. N., Williams, P. I., Gallagher, M. W., Jimenez, J. L., McDonald, A. G., Nemitz, E., Canagaratna, M. R., Jayne, J. T., Coe, H., and Worsnop, D. R.: Quantitative sampling using an aerodyne aerosol mass spectrometer: 2. Measurements of fine particulate chemical composition in two UK cities, 108, 4091, J. Geophys. Res.-Atmos., 108, 2003.

Bae, M. S., Schauer, J. J., DeMinter, J. T., Turner, J. R., Smith, D., and Cary, R. A.: Validation of a semi-continuous instrument for elemental carbon and organic carbon using a thermal-optical method, Atmos. Environ., 38, 2885–2893, 2004.
Baltensperger, U., Gäggeler, H. W., Jost, D. T., Lugauer, M., Schwikowski, M., Weingartner, E. and Seibert, P.: Aerosol climatology at the high-alpine site Jungfraujoch, Switzerland, J. Geophys. Res.-Atmos., 102, 19 707–19 715, 1997.
Baltensperger, U., Weingartner, E., Burtscher, H., and Keskinen, J.: Dynamic mass and surface area measurements, Willeke, K., and Baron, P. A., Wiley-Interscience, 2001.
Beig, G. and Brasseur, G. P.: Model of tropospheric ion composition: A first attempt, J. Geophys. Res.-Atmos., 105, 22 671–22 684, 2000.
Birch, M. E. and Cary, R. A.: Elemental carbon-based method for monitoring occupational exposures to particulate diesel exhaust, Aerosol Sci. Tech., 25, 221–241, 1996.
Bond, T. C. and Bergstrom, R. W.: Light absorption by carbonaceous particles: An investigative review, Aerosol Sci. Tech., 40, 27-67, 2006.
Canagaratna, M. R., Jayne, J. T., Jimenez, J. L., Allan, J. D., Alfarra, M. R., Zhang, Q., Onasch, T. B., Drewnick, F., Coe, H., Middlebrook, A., Delia, A., Williams, L. R., Trimborn, A. M., Northway, M. J., DeCarlo, P. F., Kolb, C. E., Davidovits, P. and Worsnop, D. R.: Chemical and microphysical characterization of ambient aerosols with the aerodyne aerosol mass spectrometer, Mass Spectrom. Rev., 26, 185–222, 2007.
Charlson, R. J., Lovelock, J. E., Andreae, M. O., and Warren, S. G.: Oceanic phytoplankton, atmospheric sulfur, cloud albedo and climate, Nature, 326, 655–661, 1987.
Cheng, Y. H. and Tsai, C. J.: Evaporation loss of ammonium nitrate particles during filter sampling, J. Aerosol Sci., 28, 1553–1567, 1997.
Chow, J. C., Watson, J. G., Crow, D., Lowenthal, D. H., and Merrifield, T.: Comparison of IMPROVE and NIOSH carbon measurements, Aerosol Sci. Tech., 34, 23–34, 2001.
Colbeck, I.: Physical and chemical properties of aerosols, Blackie Academic & Professional, London, Weinheim, New York, Tokyo, Melbourne, Madras, 1998.
Collaud Coen, M., Weingartner, E., Schaub, D., Hueglin, C., Corrigan, C., Henning, S., Schwikowski, M., and Baltensperger, U.: Saharan dust events at the Jungfraujoch: detection by wavelength dependence of the single scattering albedo and first climatology analysis, Atmos. Chem. Phys., 4, 2465–2480, 2004, http://www.atmos-chem-phys.net/4/2465/2004/.
Collaud Coen, M., Weingartner, E., Nyeki, S., Cozic, J., Henning, S., Verheggen, B., Gehrig,

R., and Baltensperger, U.: Long-term trend analysis of aerosol variables at the high alpine site Jungfraujoch, J. Geophys. Res.-Atmos., doi:10.1029/2006JD007995, 2007.
Cozic, J., Verheggen, B., Mertes, S., Connolly, P., Bower, K., Petzold, A., Baltensperger, U., and Weingartner, E.: Scavenging of black carbon in mixed phase clouds at the high alpine site Jungfraujoch, Atmos. Chem. Phys., 7, 1–11, 2007, http://www.atmos-chem-phys.net/7/1/2007/.
Evans, R. D.: The Atomic Nucleus, McGraw-Hill, N. Y., 1955.
Finlayson-Pitts, B. J. and Pitts, J. N. J.: Chemistry of the upper and lower atmosphere., Elsevier, New York, 2000.
Fuller, K. A., Malm, W. C., and Kreidenweis, S. M.: Effects of mixing on extinction by carbonaceous particles, J. Geophys. Res.-Atmos., 104, 15 941–15 954, 1999.
GAW: A Contribution to the Implementation of the WMO Strategic Plan: 2008–2011, Tech. Rep. 1384, WMO, 2007.
Henne, S., Furger, M., and Prevot, A. S. H.: Climatology of mountain venting-induced elevated moisture layers in the lee of the Alps, J. Appl. Meteorol., 44, 620–633, 2005.
Henning, S., Weingartner, E., Schwikowski, M., Gaggeler, H. W., Gehrig, R., Hinz, K. P., Trimborn, A., Spengler, B. and Baltensperger, U.: Seasonal variation of water-soluble ions of the aerosol at the high-alpine site Jungfraujoch (3580 m a.s.l.), J. Geophys. Res.- Atmos., 108, 2003.
Imhof, D., Weingartner, E., Ordonez, C., Gehrig, R., Hill, N., Buchmann, B. and Baltensperger, U.: Real-world emission factors of fine and ultrafine aerosol particles for different traffic situations in Switzerland, Environ. Sci. Tech., 39, 8341–8350, 2005.
Intergovernmental Panel on Climate Change (IPCC): Climate change 2007: The physical basis of climate change, IPCC Secretariat, Geneva, Switzerland, available at http://www.ipcc.ch; Working Group I, Final Report, available at http://ipcc-wg1.ucar.edu/wg1/wg1-report.html, 2007.
Jaklevic, J. M. and Gatti, R. C.: Beta gauge method applied to aerosol samples, Environ. Sci. Tech., 680–687, 1981.
Jayne, J. T., Leard, D. C., Zhang, X. F., Davidovits, P., Smith, K. A., Kolb, C. E., and Worsnop, D. R.: Development of an aerosol mass spectrometer for size and composition analysis of submicron particles, Aerosol Sci. Tech., 33, 49–70, 2000.
Krivacsy, Z., Hoffer, A., Sarvari, Z., Temesi, D., Baltensperger, U., Nyeki, S., Weingartner, E., Kleefeld, S., and Jennings, S. G.: Role of organic and black carbon in the chemical

composition of atmospheric aerosol at European background sites, Atmos. Environ., 35, 6231–6244, 2001.

Krueger, B. J., Grassian, V. H., Cowin, J. P. and Laskin, A.: Heterogeneous chemistry of individual mineral dust particles from different dust source regions: the importance of particle mineralogy, Atmos. Environ., 38, 6253–6261, 2004.

Lavanchy, V. M. H., Gäggeler, H. W., Nyeki, S. and Baltensperger, U.: Elemental carbon (EC) and black carbon (BC) measurements with a thermal method and an aethalometer at the high-alpine research station Jungfraujoch, Atmos. Environ., 33, 2759–2769, 1999.

Liousse, C., Cachier, H., and Jennings, S. G.: Optical and thermal measurements of black carbon aerosol content in different environments - Variation of the specific attenuation cross-section, sigma, Atmos. Environ. Part a, 27, 1203–1211, 1993.

Liu, P., Ziemann, P. J., Kittelson, D. B., and McMurry, P. H.: Generating particle beams of controlled dimensions and divergence. 1. Theory of particle motion in aerodynamic lenses and nozzle expansions, Aerosol Sci. Tech., 22, 293–313, 1995a.

Liu, P., Ziemann, P. J., Kittelson, D. B., and McMurry, P. H.: Generating particle beams of controlled dimensions and divergence. 2. Experimental evaluation of particle motion in aerodynamic lenses and nozzle expansions, Aerosol Sci. Tech., 22, 314–324, 1995b.

Maenhaut, W., Hillamo, R., Makela, T., Jaffrezo, J. L., Bergin, M. H., and Davidson, C. I.: A new cascade impactor for aerosol sampling with subsequent PIXE analysis, Nuclear Instrum. Meth B, 109, 482–487, 1996.

Malm, W. C., Schichtel, B. A., Ames, R. B., and Gebhart, K. A.: A 10-year spatial and temporal trend of sulfate across the United States, J. Geophys. Res.-Atmos., 107, 2002.

Malm, W. C., Schichtel, B. A., Pitchford, M. L., Ashbaugh, L. L., and Eldred, R. A.: Spatial and monthly trends in speciated fine particle concentration in the United States, J. Geophys. Res.-Atmos., 109, 2004.

McMurry, P. H., Wang, X., Park, K., and Ehara, K.: The relationship between mass and mobility for atmospheric particles: A new technique for measuring particle density, Aerosol Sci. Tech., 36, 227–238, 2002.

Petzold, A. and Schonlinner, M.: Multi-angle absorption photometry – a new method for the measurement of aerosol light absorption and atmospheric black carbon, J. Aerosol Sci., 35, 421–441, 2004.

Putaud, J. P., Raes, F., Van Dingenen, R., Bruggemann, E., Facchini, M. C., Decesari, S., Fuzzi, S., Gehrig, R., Huglin, C., Laj, P., Lorbeer, G., Maenhaut, W., Mihalopoulos, N., Mul-

ller, K., Querol, X., Rodriguez, S., Schneider, J., Spindler, G., ten Brink, H., Torseth, K., and Wiedensohler, A.: European aerosol phenomenology-2: chemical characteristics of particulate matter at kerbside, urban, rural and background sites in Europe, Atmos. Environ., 38, 2579–2595, 2004a.

Putaud, J. P., Van Dingenen, R., Dell'Acqua, A., Raes, F., Matta, E., Decesari, S., Facchini, M. C., and Fuzzi, S.: Size-segregated aerosol mass closure and chemical composition in Monte Cimone (I) during MINATROC, Atmos. Chem. Phys., 4, 889–902, 2004b.

Schauer, J. J., Mader, B. T., Deminter, J. T., Heidemann, G., Bae, M. S., Seinfeld, J. H., Flagan, R. C., Cary, R. A., Smith, D., Huebert, B. J., Bertram, T., Howell, S., Kline, J. T., Quinn, P., Bates, T., Turpin, B., Lim, H. J., Yu, J. Z., Yang, H., and Keywood, M. D.: ACE-Asia intercomparison of a thermal-optical method for the determination of particle-phase organic and elemental carbon, Environ. Sci. Tech., 37, 993–1001, 2003.

Schmid, H., Laskus, L., Abraham, H. J., Baltensperger, U., Lavanchy, V., Bizjak, M., Burba, P., Cachier, H., Crow, D., Chow, J., Gnauk, T., Even, A., ten Brink, H. M., Giesen, K. P., Hitzenberger, R., Hueglin, C., Maenhaut, W., Pio, C., Carvalho, A., Putaud, J. P., Toom-Sauntry, D., and Puxbaum, H.: Results of the "carbon conference" international aerosol carbon round robin test stage I, Atmos. Environ., 35, 2111–2121, 2001.

Schwikowski, M., Seibert, P., Baltensperger, U., and Gäggeler, H. W.: A study of an outstanding Saharan dust event at the high-Alpine site Jungfraujoch, Switzerland, Atmos. Environ., 29, 1829–1842, 1995.

Sharma, S., Brook, J. R., Cachier, H., Chow, J., Gaudenzi, A., and Lu, G.: Light absorption and thermal measurements of black carbon in different regions of Canada, J. Geophys. Res.-Atmos., 107, 2002.

Turpin, B. J. and Huntzicker, J. J.: Identification of Secondary Organic Aerosol Episodes and Quantitation of Primary and Secondary Organic Aerosol Concentrations During Scaqs, Atmos. Environ., 29, 3527–3544, 1995.

Verheggen, B., Cozic, J., Weingartner, E., Bower, K., Mertes, S., Connolly, P., Flynn, M., Gallagher, M., Choularton, T., and Baltensperger, U.: Aerosol activation in mixed phase clouds at the high Alpine site Jungfraujoch, J. Geophys. Res.-Atmos., doi:10.1029/2007JD008714R, 2007.

Virtanen, A., Ronkko, T., Kannosto, J., Ristimaki, J., Makela, J. M., Keskinen, J., Pakkanen, T., Hillamo, R., Pirjola, L., and Hameri, K.: Winter and summer time size distributions and densities of traffic-related aerosol particles at a busy highway in Helsinki, Atmos. Chem.

Phys., 6, 2411–2421, 2006, http://www.atmos-chem-phys.net/6/2411/2006/.
Weingartner, E., Nyeki, S., and Baltensperger, U.: Seasonal and diurnal variation of aerosol size distributions (10<D<750 nm) at a high-alpine site (Jungfraujoch 3580 m a.s.l.), J. Geophys. Res.-Atmos., 104, 26 809–26 820, 1999.
Weingartner, E., Gysel, M., and Baltensperger, U.: Hygroscopicity of aerosol particles at low temperatures. 1. New low-temperature H-TDMA instrument: Setup and first applications, Environ. Sci. Tech., 36, 55–62, 2002.
Zhang, Q., Jimenez, J. L. Canagaratna, M. R., Allan, J. D., Coe, H., Ulbrich, I., Alfarra, M. R., Takami, A., Middlebrook, A. M., Sun, Y. L., Dzepina, K., Dunlea, E., Docherty, K., DeCarlo, P. F., Salcedo, D., Onasch, T., Jayne, J. T., Miyoshi, T., Shimono, A., Hatakeyama, S., Takegawa, N., Kondo, Y., Schneider, J., Drewnick, F., Borrmann, S., Weimer, S., Demerjian, K, Williams, P., Bower, K., Bahreini, R., Cottrell, L., Griffin, R. J., Rautiainen, J. Sun, J. Y., Zhang, Y. M., and Worsnop D. R.: Ubiquity and dominance of oxygenated species in organic aerosols in anthropogenically-influenced Northern Hemisphere midlatitudes, Geophys. Res. Letter., 37, L13801, doi:10.1029/2007GL029979, 2007.
Zhang, X. F., Smith, K. A., Worsnop, D. R., Jimenez, J., Jayne, J. T., and Kolb, C. E.: A numerical characterization of particle beam collimation by an aerodynamic lens-nozzle system: Part I. An individual lens or nozzle, Aerosol Sci. Tech., 36, 617–631, 2002.
Zhang, X. Q. and McMurry, P. H.: Evaporative losses of fine particulate nitrates during sampling, Atmos. Environ. Part a, 26, 3305–3312, 1992.

Table 1. Summary of the different set of instrumentation for the different campaigns.

		March 2004	July–August 2004	February–March 2005	August 2005	Continuously measured within GAW
Mass	PM1 betameter	x	x	x	x	Since 2004
	PM1 mass derived from SMPS volume	x	x	x		
	PM1 mass derived from Scattering coefficient				x	Since 1995
	TSP betameter		x	x	x	2004–2006*
	TSP gravimetric filters	x	x	x	x	1999–2005*
Chemistry	PM1 filters	24 h	24 h	48 h	48 h	Since 1999
	TSP filters	24 h	24 h	48 h	48 h	Since 1999
	AMS	x		x		
	OC/EC Sunset analyzer			x	x	
	MAAP	x	x	x	x	Since 2003

*) A PM10 cut was added to the TSP inlet in January 2007 for the TSP betameter and in January 2006 for the TSP gravimetric filters.

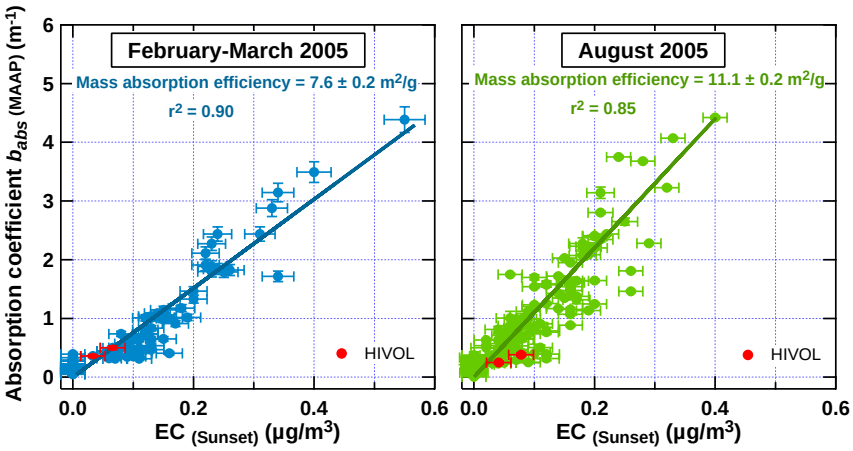

Fig. 1. Comparison of the absorption coefficient from the MAAP with the EC concentration determined by the OC/EC analyzer in February–March 2005 **(a)** and August 2005 **(b)** with 6 h averaging time. The slope represents the mass absorption efficiency.

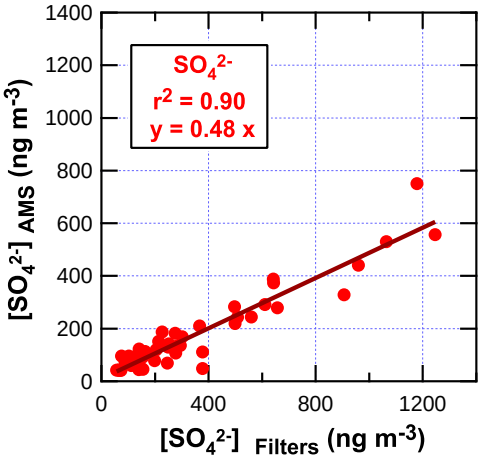

Fig. 2. Comparison of the SO_4^{-2} (PM1) concentrations measured with Q-AMS and on filters over 24 h averaging intervals in March 2004.

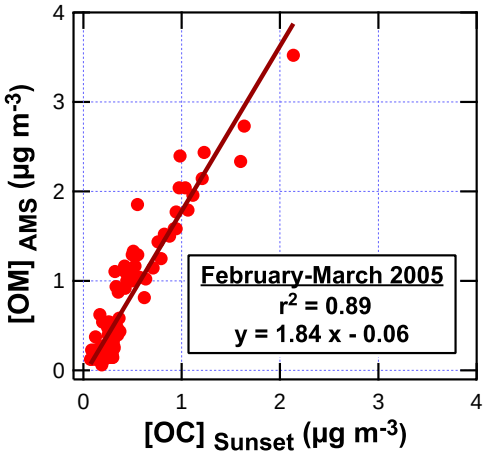

Fig. 3. Comparison of the organic mass from the Q-AMS (OM) with the organic carbon concentration from the OC/EC analyzer (OC) for February–March 2005, with an averaging time of 6 h.

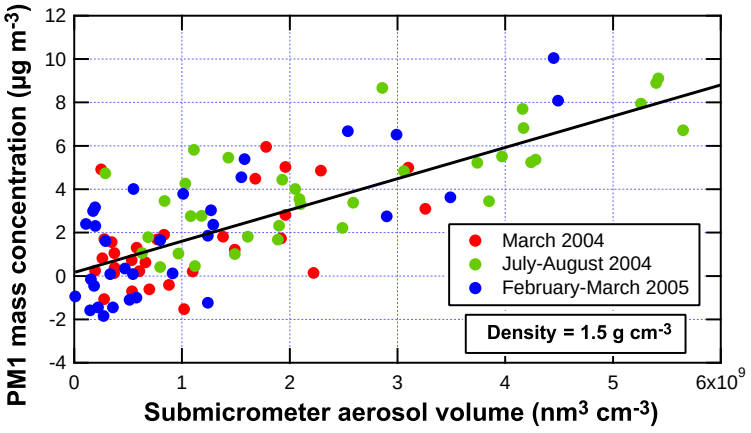

Fig. 4. Comparison of the PM1 mass concentration (betameter) with the aerosol volume concentration derived from the SMPS for winter and summer (24 h averaging time). The slope yields the effective density.

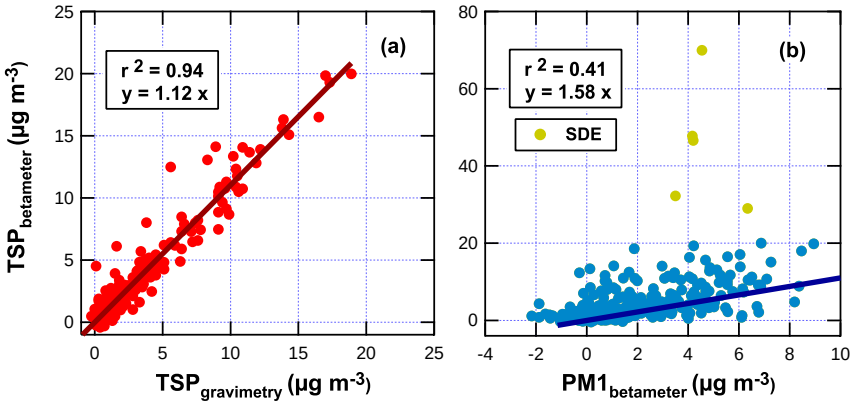

Fig. 5. Comparison of the TSP mass determined with a betameter and by gravimetry for January 2004 to January 2006 **(a)** and the TSP and PM1 mass measured with betameters for February 2004 to January 2007 **(b)** for 48 h averaging intervals.

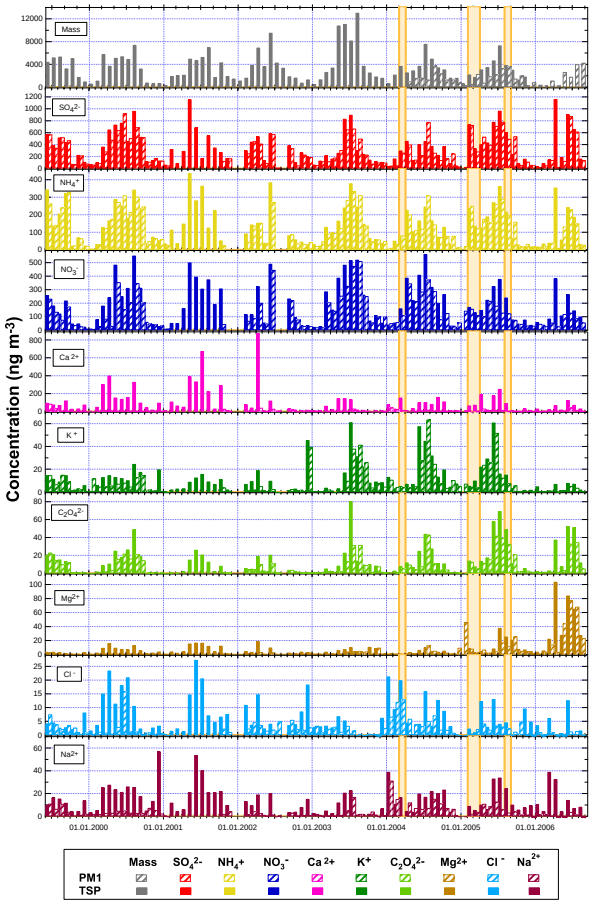

Fig. 6. Temporal evolutions of monthly averaged mass (TSP (gravimetry); PM1 (betameter) and chemical component concentrations (filters) for the period June 1999 to September 2006. Orange bands represent the time periods when further information on chemical composition was measured during intensive field campaigns.

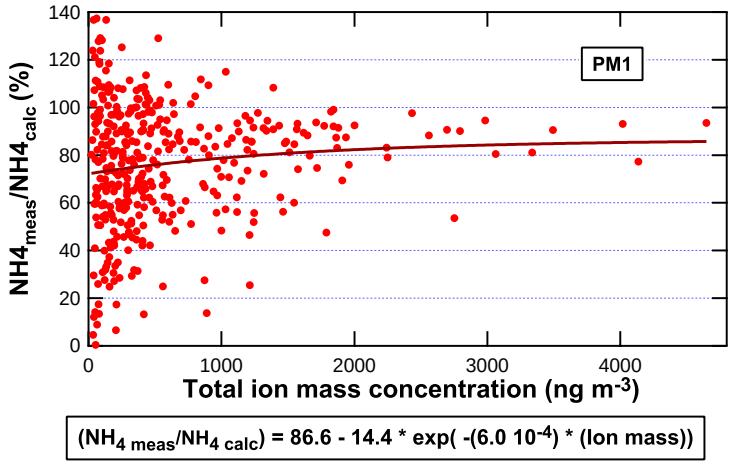

Fig. 7. Ratio of the measured NH_4 mass to the NH_4 calculated to reach neutralization (i.e. formation of NH_4NO_3;$(NH_4)_2SO_4$) as a function of the total ion mass concentration for PM1 measured with filters (daily averages). The exponential fitted line is also presented.

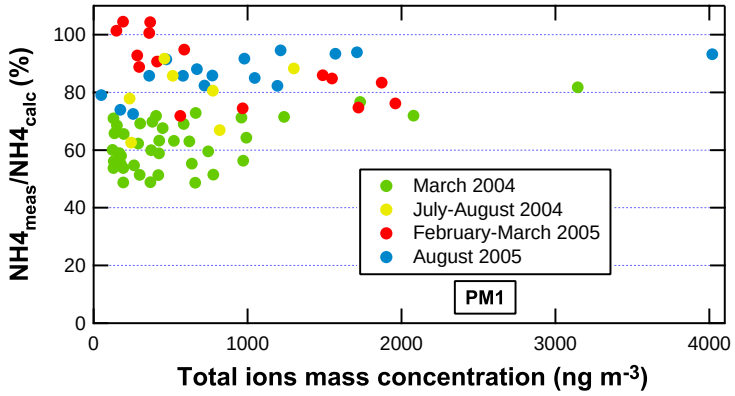

Fig. 8. Ratio of the NH_4 mass to the NH4 calculated to reach neutralization (i.e. formation of NH_4NO_3;$(NH_4)_2SO_4$) as a function of the total ion mass concentration for PM1 during the intensive campaigns (daily averages).

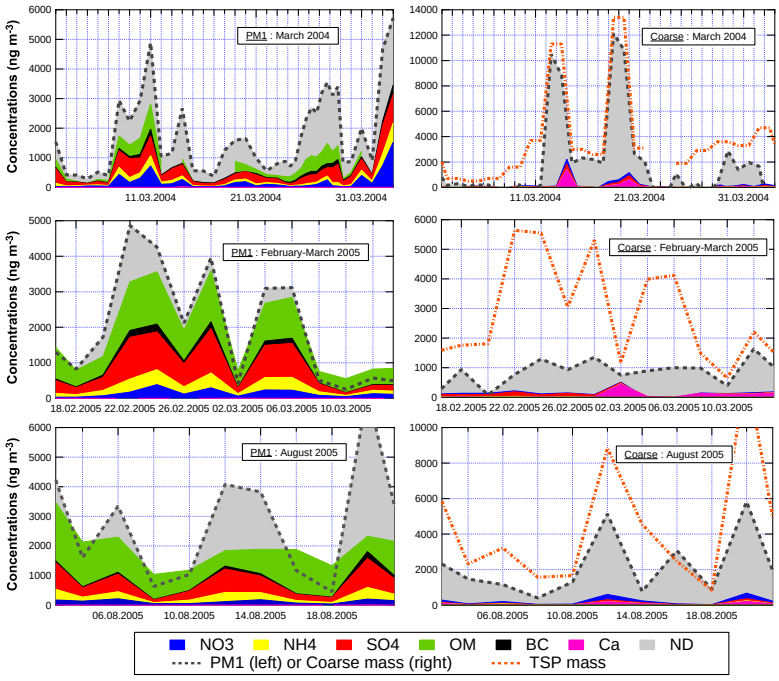

Fig. 9. Time series of the chemical composition of PM1 (left) and the coarse mode (right) for March 2004, February–March 2005, and August 2005. Inorganic composition was measured with filters, BC was measured with a MAAP and OM fraction was measured with an OC/EC analyzer (except for March 2004 where OM data are from a Q-AMS). PM1 mass was derived from SMPS (except for August 2005 where it was deduced from the aerosol scattering coefficient at 450 nm). TSP mass were measured with a betameter (except for March 2004 where data are from gravimetric measurement).

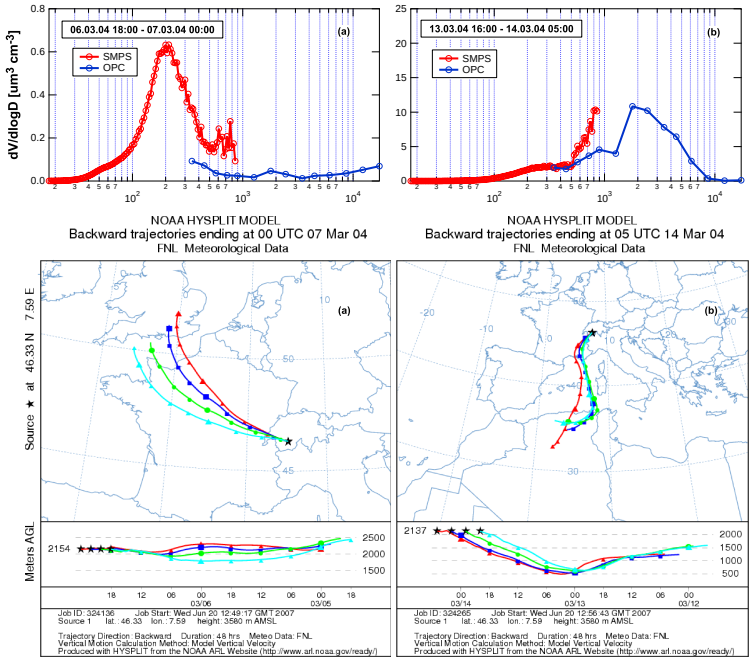

Fig. 10. Top: Size distributions measured with an SMPS for diameters below 800 nm and with an OPC for diameters above 300 nm (not corrected). Bottom: back-trajectories calculated with the NOAA HYSPLIT model for two periods without **(a)** and with **(b)** influence of mineral dust.

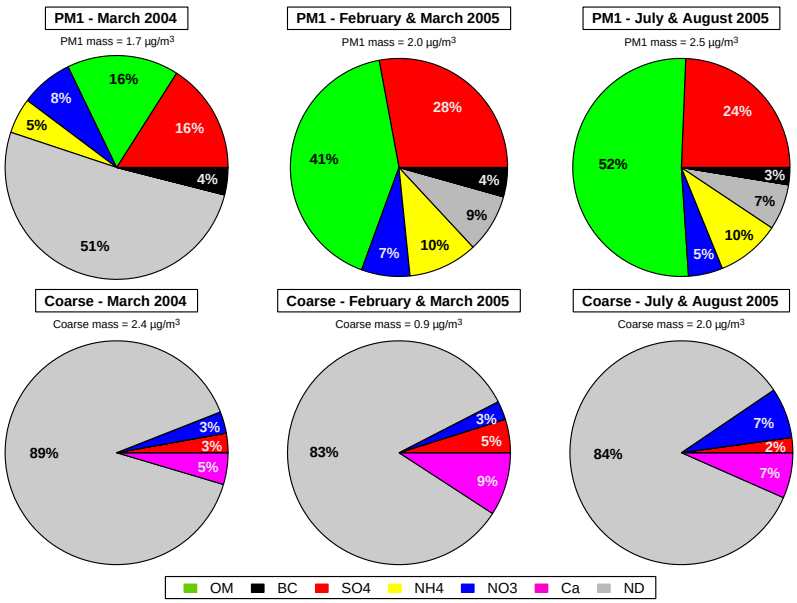

Fig. 11. Mass closure of PM1 and coarse mode for the three campaigns. See text and Table 1 for details on the employed instrumentation.